POINT SPREAD FUNCTION ESTIMATION AND UNCERTAINTY QUANTIFICATION

By

Kevin Thomas Joyce

B.S., Montana State University, Bozeman, MT, 2006
M.S., Montana State University, Bozeman, MT, 2009

Dissertation

presented in partial fulfillment of the requirements
for the degree of

Doctorate of Philosophy
in Mathematics

The University of Montana
Missoula, MT

May 2016

Approved by:

Sandy Ross, Associate Dean of the Graduate School
Graduate School

Dr. Johnathan Bardsley, Co-Chair
Mathematical Sciences

Dr. Aaron Luttman, Co-Chair
Signals Processing and Applied Mathematics
National Security Technologies, LLC, Las Vegas, NV

Dr. Jon Graham
Mathematical Sciences

Dr. Leonid Kalechev
Mathematical Sciences

Joyce, Kevin, Doctorate of Philosophy, May 2016   Mathematics

Point Spread Function Estimation and Uncertainty Quantification

Committee Chair: Johnathan Bardsley, Ph.D.

Acknowledgments

Notations

Contents

List of Tables

List of Figures

Chapter 1

Introduction

In addition to being a rich source of artistic and creative inspiration, pictures, or more precicely visual data, have been a crucial source of scientific information. Even the word "observation" generally connotes close visual scrutiny, and its use as a catch-all for the measured verification of a hypothesis exemplifies the central role of visual perception in science. Many important scientific results have used visual data to discover and explain natural phenomena; for example, visual observations such as the color and shape of various plant organs in Gregor Mendel's famous experiments on hybridized peas formed the primary source of data for developing his famous model for genetic inheritance [**?**]. Arthur Eddington's famous celestial observations in the early 20th century, which provided the first experimental evidence supporting Albert Einstein's general theory of relativity, recorded the gravitationally lensed path of a comet on photographs taken during a solar eclipse [**?**]. Yet, in these cases, only the *qualitative* components of the visual response and their relationship to the experiment were relevant. With the advent of the camera, photosensitive chemistry, and later digital imaging technology, high-fidelity recording of visual observations became possible, allowing the potential to *quantitatively* analyze visual information. The ever-progressing technology in optical science and engineering are rapidly increasing the amount of data that can be measured in an image;

yet, it is precisely this extreme density of data that makes a quantitative analysis challenging.

Images, when viewed quantitatively, can be described as the response of the incidence of light and the subsequent exchange of energy on a grid of regularly spaced points, which we refer to as pixels. The raw volume of recorded data is usually very large. For instance, astronomical images such as those captured by interstellar robotic probes are digitized on a pixel grid typically 800×800 or higher, that measures the counts of captured photons on an array of detectors referred to as a charged coupled device (CCD) array [Showalter et al., 2006]. In medical imaging, computed tomography is an imaging process whereby a three dimensional image is constructed from a series of axial measurements of attenuation of electromagnetic radiation. The additional dimension to the grid multiplicatively increases the data. Of primary focus in this work are pulsed X-ray measurements, referred to as radiographs, that are used as an experimental diagnostic of high-energy physics experiments. In this case, X-rays are pulsed through a contained experiment, then the attenuated X-rays excite a crystal that responds by luminescing visible light at an intensity related directly to the energy of the attenuated wavefront. The light is then captured on a high resolution CCD array on the order of 1028×1028 pixels.

A quantitative analysis of image data must take into account pixel-to-pixel dependence. That is, the measured values at one pixel depends heavily on adjacent or neighboring pixels, thus, one expects the measured data to be highly correlated. From a statistical point of view, explicitly accounting for spatial correlation in data is a very complex problem, and one of the first substantive achievements was by Julian Besag in 1974 with his seminal paper "Spatial Interaction and the Statistical Analysis of Lattice Systems," [Besag, 1974]. The relatively recent date of this publication (in mathematical terms) coupled with the prevalence of image data prior to this, hints that the requisite tools for a rigorous statistical analysis require modern mathematical theory and state of the art computation. The development over the past several decades in this area has inspired a wealth of theory and computational tools, but is far from complete. Moreover, a broad field of scientific disciplines have considered

image data, or more generally spatially correlated data, in one way or another; fields such as astronomy, astrophysics, biology, medicine, geology, computer science, and nuclear physics to name a few. Each have a unique perspective on the problem, and a vast literature on the subject has accumulated. See [Cressie, 1993] and the references therein. Although much work has been done, it is still a very active research area and is far from the level of consensus and understanding that analysis of independently sampled data has achieved. But it is precisely this lack of independence that makes an image interesting – independent image data is "gray noise" from which one can only infer the average of the measured pixels. The aim of this work is to develop and adapt current models and methods for estimation and quantifying uncertainty to a small component of image analysis related specifically to the *system for capturing images.* Understanding this component is an important preliminary step to developing methods for quantitatively analyzing the images themselves.

1.1 Modeling blur with a PSF

One major component of the spatial relationship of neighboring pixels of an image is due to blur from the imaging instrumentation. That is, under the assumption that arbitrary images are measured by a consistently modeled system, what contribution does this system have on how pixels are related, and how can we quantify this relationship? A widely used model for blurring [Hansen, 2010, Jain, 1989, Vogel, 2002, Epstein, 2008] expresses this relationship through a point-wise integral product with a function that describes interaction with neighboring points, e.g.

$$b(x,y) = \iint_\Omega k(x,y;s,t)f(s,t)\,dsdt \tag{1.1}$$

where $b(x,y)$ are the quantitative measurements of the blurred image, $f(s,t)$ represents the ideal un-blurred image with domain Ω, and k is a function that describes the blur for each (x,y). Informally, the function "weights" the other points in the image, and the integration "averages" the weighted values of the ideal image $f(s,t)$. The form of the weighting function

is guided by optical principles and the physics of the system that generally dictate that, for fixed (x, y), $k(x, y; \cdot, \cdot)$ is concentrated (in the measured or integrated sense) at (x, y) and continuously decays as the distance from (s, t) to (x, y) increases. In this sense, the weighting effect of (1.1) "spreads" outward from (x, y), hence, is referred to as a point spread function (PSF). The function in (1.1) is often interpreted as a family of PSFs $k(x, y; \cdot, \cdot)$ indexed at each (x, y).

Under the additional assumption that the effect of blur is invariant to translations of (x, y), the dimension of the domain of the PSF reduces from four to two (we still denote it by k) and blur at (x, y) is given by integrating against translates of $k(x, y)$, i.e.

$$b(x, y) = \iint_{\Omega} k(x - s, y - t) f(s, t) \, ds dt. \tag{1.2}$$

The integral product in (1.1) is called the convolution of f by k. The assumptions for modeling blur in this form are quite common, and methods that mitigate the effect of blur are often referred to as deconvolution techniques. Note that a change of variables by $s' = x - s$ and $t' = y - t$ results in a convolution of k by f, which is to say that convolution, as an operation, is symmetric. This dual relationship between the PSF and the image will allow us to use the framework and tools of deconvolution for the problem of PSF estimation.

Typically, deconvolution methods assume that the form of the PSF can be accurately described by modeling the imaging system [Jain, 1989, **?**], but for complex imaging systems such as the one described for X-ray radiography, this is not realistic. Instead, if the imaging system is designed so that repeated images can be taken under consistent conditions, then by convolution symmetry, the blurring of a *known calibration image* can be cast as deconvolving the PSF from the ideal f corresponding to the known image.

A direct estimate can be obtained by imaging a bright point source, which approximates the impulse response to (1.2). In astronomical imaging, the point source can be a bright distant

star, or in a controlled setting where visible light is measured, a focused laser beam provides a good point source estimate. However, in the spectral regime of high-frequency X-rays, the problem of focusing high frequency-light is notoriously difficult and usually is impractical in situations of interest, so a point source estimate of the PSF is usually unavailable at these frequencies. Instead, the system response of a uniformly opaque calibration object with a simple geometry can be measured. Under the assumption that the object attenuates X-rays sufficiently so that the ideal image is given by an indicator function for a known set $E \subseteq \Omega$, one can form a deconvolution problem that exploits our control over the geometry of E. When the calibration object is a vertical edge at a known and fixed location in the imaging plane, then E is the half plane, and its characteristic function depends only on s and is given by $f(s) = 1$ if $s \geq 0$ and $f(s) = 0$ if $s < 0$. The model for blur in 1.2 reduces to

$$b(x) = \iint_{\Omega} k(s,t) f_E(x - s) ds dt. \tag{1.3}$$

Note that b no longer depends on y, hence the model output provides data only in the horizontal dimension. This leads to the problem of estimating k from b in (1.3) being underdetermined, since there are generally many distinct k that can result in the same output b. An additional assumption of *radial symmetry* on k will sufficiently constrain the problem and is addressed in the following section.

1.2 Edge blur by a radially symmetric PSF

A large part of designing a system for imaging is to minimize the effect of blur. Often, limitations due to physical laws put a lower bound on the measurement precision so that even an optimal design cannot ignore the effect of blur. Although arbitrary resolution may be impossible, engineering effort can still optimize accuracy, or, equivalently, minimize bias. Hence, an optimally designed imaging system should exhibit isotropic blur (an absence of

direction bias), so that, in the convolution model, the PSF is radially symmetric. In fact, many parametrically modeled PSFs assume radially symmetry [Doering et al., 1992, Jain, 1989, Kundur and Hatzinakos, 1996a, Watson, 1993].

When one assumes that the PSF of their system is radially symmetric, then it has a unique one-dimensional representation. That is, there exists a function p defined on $\Omega_1 \subseteq (0, \infty)$ so that $k(s, t) = p\left(\sqrt{s^2 + t^2}\right)$. The function p is referred to as the radial profile of k. When Ω is almost all of $\mathbb{R}^2$ (in the sense of measure), then substituting p into (1.3) gives

$$
\begin{aligned}
b(x) &= \int_{-\infty}^{x} \left(\int_{-\infty}^{\infty} p\left(\sqrt{s^2 + t^2}\right) dt \right) ds \\
&\stackrel{\text{def}}{=} \int_{-\infty}^{x} \ell(s) ds.
\end{aligned}
\tag{1.4}
$$

The function $\ell(s)$ is the integration along a line perpendicular to the edge E, and its form is commonly encountered in tomographic imaging science. The collection of line integrals parametrized by their angle of incidence is called the Radon transform of k, and when k is radially symmetric, the transform is completely determined by a single projection. In this special case, the operator that takes the radial profile p to l is called the Abel transform. In Epstein [2008], the following explicit expression for obtaining p, given ℓ is derived;

$$
p(r) = -\frac{1}{\pi r} \frac{d}{dr} \left(\int_{r}^{\infty} \frac{\ell(s) s \, ds}{(s^2 - r^2)^{1/2}} \right).
\tag{1.5}
$$

To see this, we can express the inner integral in (1.4) as

$$
\ell(s) = 2 \int_{|s|}^{\infty} \frac{p(t) t}{(t^2 - s^2)^{1/2}} dt
\tag{1.6}
$$

by symmetry of the integrand (it is even) and a change of variable by $r = s^2 + t^2$. Now,

interchanging the order of integration in (1.5) results in

$$\left(\int_r^\infty \frac{\ell(s)s\,ds}{(s^2 - r^2)^{1/2}} \right) = \int_r^\infty \int_s^\infty \frac{p(t)ts}{(s^2 - r^2)^{1/2}(t^2 - s^2)^{1/2}}\,dt\,ds$$

$$= \int_r^\infty p(t)t \int_r^t \frac{s}{(s^2 - r^2)^{1/2}(t^2 - s^2)^{1/2}}\,ds\,dt. \tag{1.7}$$

Another change of variables by $s^2 = \tau t^2 + (1 - \tau)r^2$ (note $s \geq 0$) so that the inner integral in (1.7) is

$$\int_r^t \frac{s}{(s^2 - r^2)^{1/2}(t^2 - s^2)^{1/2}}\,ds = \frac{1}{2} \int_0^1 \frac{1}{\tau^{1/2}(1 - \tau)^{1/2}}\,d\tau. \tag{1.8}$$

Note that the resulting integral is independent of both r and t, thus, is constant. To evaluate it, recall the Gamma function identity

$$\frac{\Gamma(\alpha)\Gamma(\beta)}{\Gamma(\alpha + \beta)} = \int_0^1 \tau^{-\alpha}(1 - \tau)^{\alpha - 1}\,d\tau, \tag{1.9}$$

from which the expression in (1.8) reduces to $\pi/2$. Collecting these results and applying the fundamental theorem of calculus with the assumption that $\lim_{r \to \infty} p(r) = 0$, proves the identity in (1.5).

With this result, p can be analytically recovered from b in (1.4). That is, given $b(x)$, the fundamental theorem of calculus gives $\ell(s)$ by differentiating $b(x)$, then applying the inversion formula in (1.5) to $b'(x)$ gives the radial profile $p(r)$. Hence, the assumption of radial symmetry sufficient constrains the problem to uniquely determine the PSF form an edge calibration object illustrated in Figure 1.3.

In theory, we have outlined a solution to the problem, but there is one more component to the model that has not been addressed – random effects due to measurement error – for which a direct application of outlined method on measured data will fail spectacularly, due to the estimation problem being "ill-posed" which we address in the next section.

1.3   PSF reconstruction as an ill-posed inverse problem

The measurements of the imaging system are generally not deterministic and are subject to measurement noise. Precisely modeling the stochastic effect of measurement error is system dependent and can be quite complicated. In the X-ray radiography example, uncertainty can enter into the system at the luminescing crystal response, at the counts of CCD array, or through the electrical transmission of the signal. In order to be broadly applicable, and appealing generally to various central-limit-theorem-like results in probability [Durrett, 2010], we model the stochastic measurement effect in aggregate as an additive, independent Gaussian noise process with zero mean and unknown variance. For now, this assumption can be viewed as a small perturbation from the model, but its form will be important for the inference techniques developed in subsequent chapters.

Estimating a quantity of interest, in our case k, from indirect and noisy measurements, b, with a model where an operator takes k *to* b (referred to as the *forward operator*) is called an inverse problem. The problem is called well-posed when the forward operator is invertible, and the inversion is insensitive to small perturbations. These famous conditions were laid out by Jacques Hadamard in the early 20th century [**?**], but a number of important applications have arisen (among those computational imaging) where these conditions are violated, enough to the extent that the term "inverse problems", as it refers to the mathematical research area, is exclusively devoted to solving these *ill-posed* problems. In particular, most cases of interest exhibit a model where the inverse of the forward operator is very sensitive to perturbations.

The discussion thus far for PSF reconstruction has been somewhat informal, as we have not defined a space for the PSF or its radial representation, so we have not formally defined a model forward operator. Defining these spaces in detail is somewhat technical and will be addressed in in Chapter 2; however, assuming these spaces have been defined, we can illustrate that the problem of reconstructing the radial profile is ill-posed.

A change of variables in the forward model (1.3) (again assuming Ω is full measure in $\mathbb{R}^2$) by $(s,t) = T(r,v) = (r\cos v, r\sin v)$, has $|dT(r,v)| = r$ and

$$
\begin{aligned}
b(x) &= \int_0^\infty p(r) \left(\int_{-\pi}^{\pi} f_E(x - r\cos v) dv \right) r\, dr \\
&= \int_0^\infty p(r) g(x,r) r\, dr,
\end{aligned}
\tag{1.10}
$$

where

$$
g(x,r) \stackrel{\text{def}}{=} \begin{cases} 0 & x < -r \\ 2(\pi - \text{acos}(x/r)) & |x| < r \\ 2\pi & x > r \end{cases}
\tag{1.11}
$$

To see that g has this form, note that integrating $f_E(x - r\cos v)$ is the radian measure of the set $\{v \in (-\pi, \pi) : r\cos v \leq x\}$; see Figure 1.1. There are two key observations to make. First note that $g(x,r)$ is continuous (although it has a discontinuity in its partial derivatives across $r = s$). Second is that the graph of $b(x)$ exhibits reflection symmetry about $b(0)$. To see this analytically, for $x > 0$ the formulation in terms of the Abel transform in (1.4) gives

$$
\begin{aligned}
b(x) &= \int_{-\infty}^0 \ell(s)ds + \int_0^x \ell(s)ds \\
&= b(0) - \int_0^{-x} \ell(s')ds' \\
&= b(0) - b(-x).
\end{aligned}
\tag{1.12}
$$

So, $b(x)$ defined on either $(-\infty, 0]$ or $[0, \infty)$ completely determines p.

With these observations, if $G : \mathcal{H}_1 \to \mathcal{H}_2$ is an operator between closed isometric subspaces of $L^2([0,\infty))$ that acts by the integral equation in (1.10), then G is a compact Hilbert-Schmidt operator. Thus, the spectral theory for such operators implies that G has a countable spectrum that has zero as a limit point, hence, the inverse is unbounded, which results in an ill-posed problem. See one of many texts on functional analysis [Bachman and Narici, 1966, Rudin, 1991] and [Tikhonov, 1963, Vogel, 2002, Morozov and Stessin, 1993] for the analytic treatment
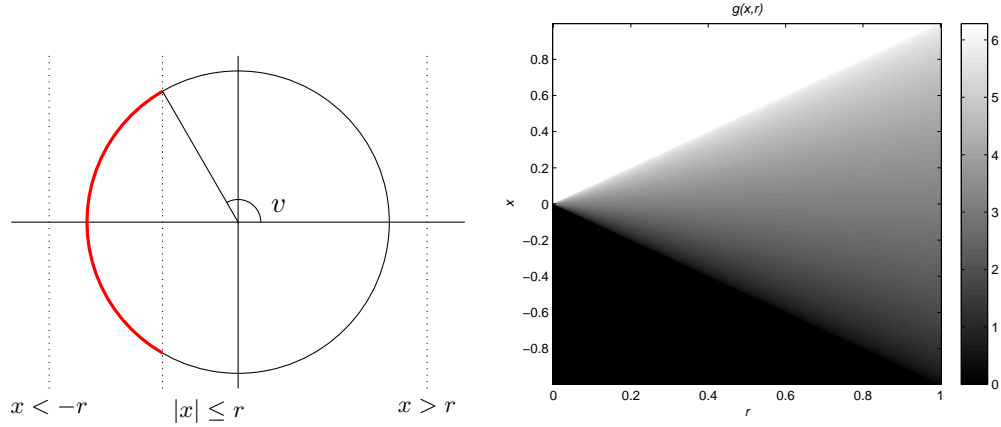
Figure 1.1: The PSF forward integral operator kernel $g(x, r)$ represented as the arc measure of v in $(-\pi, \pi)$ where $x \geq r \cos v$.

of ill-posed problems.

Solving ill-posed inverse problems requires *regularization* of the unbounded inverse. Recall that the original formulation of the problem is cast in terms of deconvolution, and much of the literature of inverse problems is devoted to this subject. This work draws heavily from techniques for that purpose. In particular, we will take a Bayesian approach to the inverse problem so that in addition to estimating k, uncertainties in the estimate can quantified by analysing the posterior distribution. These methods have been the subject of much recent research (see the books [Calvetti and Somersalo, 2007, Kaipio and Somersalo, 2005, Stuart, 2010]), and the problem of PSF reconstruction fits neatly into that framework once the spaces $\mathcal{H}_1$ and $\mathcal{H}_2$ have been defined.

1.4 Organization

In the next chapter, we will give a basic outline of Bayesian estimation techniques for the problem of PSF reconstruction. Primarily, we will develop the theoretical framework of how inference can be carried out on the radial profile of the PSF, when prior assumptions are placed
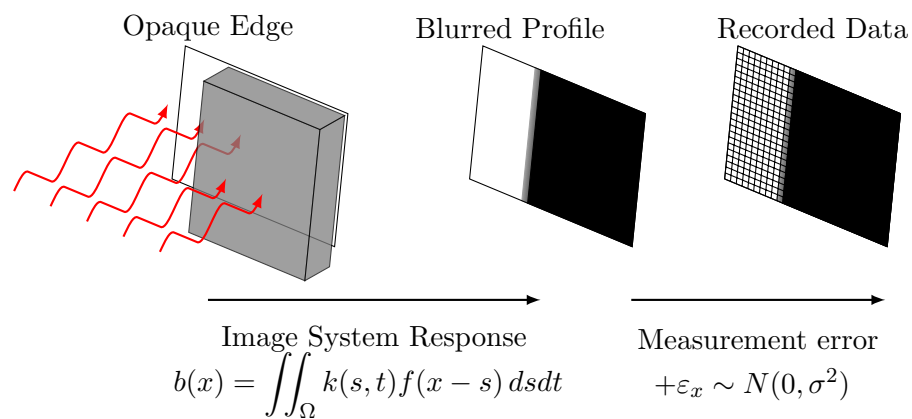
Figure 1.2: A schematic of the measurement model for an X-Ray image of an edge. An opaque block aligned with the imaging plane blocks light on the half plane to produce a blurred edge.
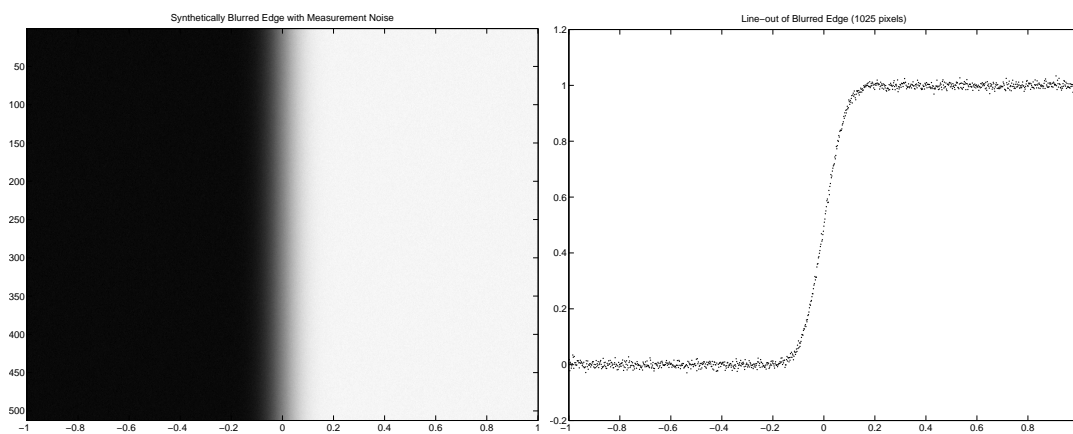

Figure 1.3: A synthetically blurred edge with simulated measurement error and a line-out (horizontal cross-section) from the data.

on the PSF itself. Chapter 2 will be mainly theoretical, but the explicit forms for the discrete model of the forward operator and prior are motivated and derived there. Chapter 3 will give details on how to carry out the estimation on a computer. There, we will deal with how to discretely represent each of the necessary components in the estimation problem. We will also motivate and present the design of a detailed algorithm for carrying out the estimation outlined in Chapter 2. Finally, in Chapter 4, we present the results of an implementation on synthetically derived data and on measured data from a high-energy X-ray imaging system at the U.S. Department of Energy's Nevada National Security Site. We will end with a discussion of conclusions and possible future work.

Bibliography

Milton Abramowitz and Irene Stegun. *Handbook of Mathematical Functions*. Dover, 9 edition, 1972.

George Bachman and Lawrence Narici. *Functional Analysis*. Academic Press, 1966.

Julian Besag. Spatial interaction and the statistical analysis of lattice systems. *Journal of the Royal Statistical Society. Series B (Methodological)*, pages 192–236, 1974.

R. Bracewell. *The Fourier Transform and Its Applications*. McGraw-Hill, 1965.

Daniela Calvetti and Erkki Somersalo. *An Introduction to Bayesian Scientific Computing: Ten Lectures on Subjective Computing*, volume 2. Springer Science & Business Media, 2007.

Noel AC Cressie. *Statistics for spatial data*. Wiley New York, 1993.

Giuseppe Da Prato. *An introduction to infinite-dimensional analysis*. Spriner Science & Business Media, 2006.

Edward R. Doering, Joseph Gray, and John P. Basart. Point spread function estimation of image intensifier tubes. *Review of Progress in Quantitative Nondestructive Evaluation*, 11: 323–329, 1992.

Richard Durrett. *Probability: theory and examples*. Cambridge university press, 2010.

Charles L. Epstein. *Introduction to the Mathematics of Medical Imaging.* Society for Industrial and Applied Mathematics, 2008. ISBN 9780898716429.

Ruggeri Fabrizio, Michael P Wiper, and David Rios Insua. *Bayesian analysis of stochastic process models.* Wiley, 2012.

David H Griffel. *Applied functional analysis.* Courier Corporation, 2002.

P. C. Hansen. *Discrete Inverse Problems: Insight and Algorithms.* SIAM, Philadelphia, 2010.

P.C. Hansen. Numerical tools for analysis and solution of Fredholm integral equations of the first kind. *Inverse Problems*, 8:956–972, 1994.

P.C. Hansen, J.G. Nagy, and D.P. O'Leary. *Deblurring Images: Matrices, Spectra, and Filtering.* SIAM, Philadelphia, 2006.

Lars H ormander. *The analysis of linear partial differential operators I.* Springer-Verlag, 1983.

V. Hutson and J. S. Pym. *Applications of Functional Analysis and Operator Theory*, volume 146 of *Mathematics in Science and Engineering.* Academic Press, 1980.

A.K. Jain. *Fundamentals of Digital Image Processing.* Prentice-Hall information and system sciences series. Prentice Hall, 1989.

Warren P. Johnson. The curious history of fa di brunos formula. *Amer. Math. Monthly*, 109: 217–234, 2002.

J. Kaipio and E. Somersalo. *Statistical and Computational Methods for Inverse Problems.* Springer, 2005.

O. Knill, R. Dgani, and M. Vogel. A new approach to abel's integral operator. *Astronomy and Astrophysics*, 274:1002–1008, 1993.

D. Kundur and D. Hatzinakos. Blind image deconvolution. *IEEE Signal Processing Magazine*, 13(3):43–64, 1996a.

D. Kundur and D. Hatzinakos. Blind image deconvolution revisited. *IEEE Signal Processing Magazine*, 13(6):61–63, 1996b.

Vladimir Aleseevich Morozov and Michael Stessin. *Regularization methods for ill-posed problems.* CRC Press, 1993.

Keith W Morton and David Francis Mayers. *Numerical solution of partial differential equations: an introduction.* Cambridge university press, 2005.

Y.P. Pyt'ev. Methods of reduction of measurements in Hilbert spaces. *Mathematics of the USSR-Sbornik*, 54(2):525–549, 1986.

Walter Rudin. *Functional analysis. International series in pure and applied mathematics.* McGraw-Hill, Inc., New York, 1991.

S. Särkkä. Linear operators and stochastic partial differential equations in gaussian process regression. In *Artificial Neural Networks and Machine Learning-ICANN 2011*, pages 151–158. Springer, 2011.

MR Showalter, MK Gordon, and D Olson. Vg1/vg2 saturn iss processed images v1.0. NASA Planetary Data System, 2006.

Robert S Strichartz. *The way of analysis.* Jones & Bartlett Learning, 2000.

A. M. Stuart. Inverse problems: A bayesian perspective. *Acta Numerica*, 19:451–559, 2010.

A.N. Tikhonov. Regularization of incorrectly posed problems. *Soviet Mathematics Doklady*, 4:1624–1627, 1963.

C.R. Vogel. Stochastic inversion of linear first kind integral equations. ii. discrete theory and convergence results. *Journal of Integral Equations*, 7:73–92, 1984.

Curtis R. Vogel. *Computational Methods of Inverse Problems.* Society for industrual and applied mathematics, 2002.

Scott A. Watson. Real-time spot size measurement for pulsed high-energy radiographic machines. *Proceedings of the 1993 Particle Accelerator Converence*, 4:2447–2449, 1993.